

NEUTRAL ENERGY PRODUCTION IN e^+e^- ANNIHILATION

Daniel L. Scharre
Stanford Linear Accelerator Center
Stanford University, Stanford, California 94305

Abstract: Recent results from SPEAR on inclusive γ and π^0 production in e^+e^- annihilation are presented. These results are inconsistent with expectations based on an earlier analysis of charged particle production in e^+e^- annihilation (assuming all-pion production). A new analysis which incorporates production of heavy particles, resonances, and τ 's is presented which adequately describes the available charged and neutral data.

Résumé: Des résultats récents de SPEAR concernant la production inclusive de γ et π^0 par annihilation e^+e^- , sont présentés. Ces résultats ne sont pas consistants avec les prévisions basées sur des analyses antérieures de production des particules chargées dans les annihilations e^+e^- (en supposant une production uniquement de pions). Une analyse nouvelle incorporant une production de particules lourdes, de résonances et de τ est présentée ici; cette analyse décrit les données chargées et neutres qui existent aujourd'hui.

Presented at the 14th Rencontre de Moriond, Les Arcs, France,
March 11 - 23, 1979.

* Work supported by the Department of Energy under contract number EY-76-C-03-0515.

I. Introduction

A previous analysis of inclusive charged particle production in e^+e^- annihilation based on data from the SLAC-LBL Mark I magnetic detector at SPEAR accounted for approximately half of the produced energy in terms of charged particle production for center-of-mass energies above 5 GeV.¹⁾ It has been generally assumed that the majority of the remaining energy goes into neutral particle production. Recent results from the Lead-Glass Wall experiment at SPEAR which measured inclusive γ and π^0 production between 4.9 and 7.4 GeV indicate that production of π 's and γ 's is consistent with only half the charged- π production.²⁾ These results appear to be somewhat inconsistent. In this talk, I will first review the data from the Lead-Glass Wall experiment, and then present the results of an analysis of the data which describes both the charged and neutral particle distributions without inconsistencies.

II. Detector

The data were collected with the Stanford Linear Accelerator Center-Lawrence Berkeley Laboratory magnetic detector at SPEAR.³⁾ γ 's are detected using a system of lead-glass counters (referred to as the LGW) which replaces one octant of the magnet return yoke and covers a solid angle of approximately $0.053 \times 4\pi$ sr.⁴⁾ The detector is shown in Fig. 1. The LGW consists of two arrays of lead-glass

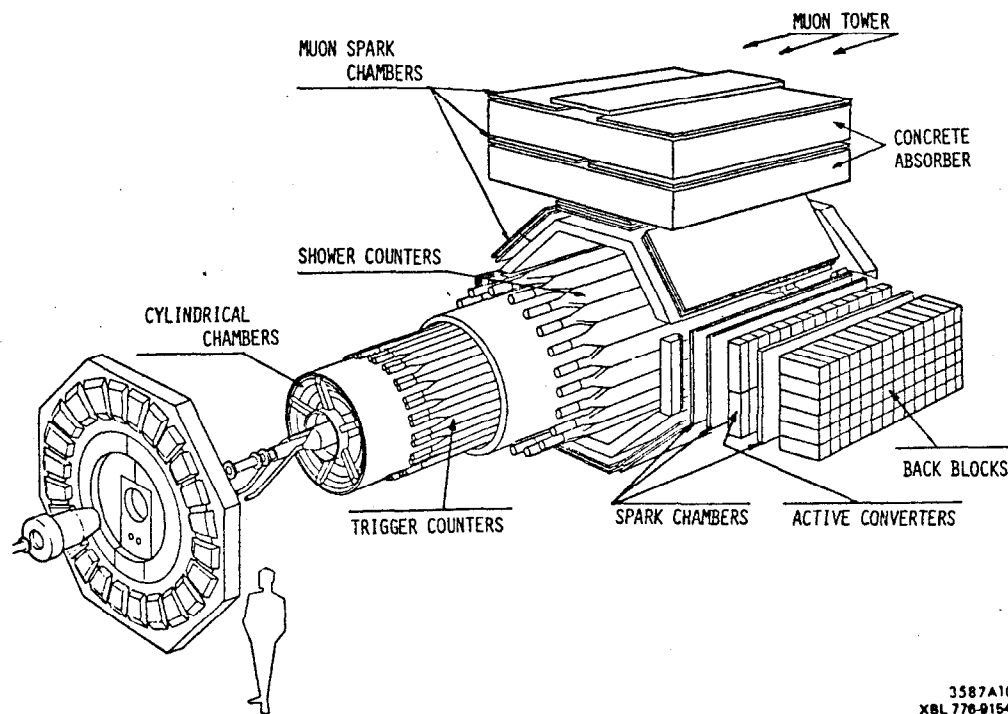


Fig. 1. SLAC-LBL magnetic detector with the Lead-Glass Wall addition.

blocks (a 2×26 array of 10×90 -cm² blocks, 3.3 radiation lengths thick, and a 14×19 array of 15×15 -cm² blocks, 10.5 radiation lengths thick) and three planes of magnetostrictive spark chambers outside the 1-radiation length aluminum coil.

γ 's are identified by correlated energy deposits in the lead-glass blocks and tracks in the spark chambers which are not associated with charged particles detected in the central detector. γ 's which convert in the coil (as identified by tracks in the two spark-chamber planes situated between the coil and the inner plane of lead-glass blocks) are corrected for the average energy loss (approximately 50 MeV). The γ energy resolution is $\Delta E/E \approx 0.09/E^{1/2}$ (E in GeV), and the angular resolution is $\Delta \theta \approx 0.5^\circ$. The γ efficiency (for γ 's going into the wall) is essentially 100% for γ 's with energy above 150 MeV.

π^0 identification is accomplished by combining pairs of γ 's in the LGW. A background subtraction is made to statistically extract the π^0 peak. The π^0 acceptance is shown in Fig. 2. The maximum acceptance is 2%. The decrease in acceptance with momentum (above approximately 1.5 GeV/c is due to resolution problems in separating γ 's from small opening angle π^0 decays.

III. Inclusive Cross Section Measurements

The LGW analysis was based on a sample of 50,000 multiprong events (events with three or more prongs) in the center-of-mass energy (E_{cm}) range from 4.9 to 7.4 GeV. The inclusive γ cross section was measured independently in each of the three different center-of-mass energy regions shown in Table I. Corrections to the data were made for trigger efficiency, geometric acceptance, initial-state radiation, and beam-gas background.

Figure 3 shows the inclusive γ cross section $s d\sigma/dx$, as a function of x for γ 's in the E_{cm} range from 4.9 to 7.4 GeV. (In all cases, x will be defined to be the particle momentum divided by the

beam energy.) All errors shown are statistical with the exception of the lowest two data points, where the error has been increased to account for the uncertainty in the background. (In ref. 2, the data is plotted separately for each of the

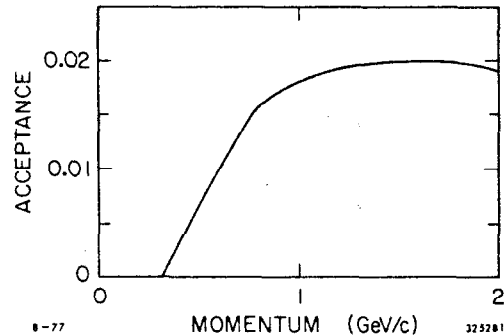


Fig. 2. π^0 acceptance in the LGW as a function of π^0 momentum for isotropically produced π^0 's.

E_{cm} (GeV)	$\int \mathcal{L} dt (nb^{-1})$	Number of Hadrons
4.9 - 6.0	1300	11,000
6.0 - 6.9	2800	19,000
6.9 - 7.4	3400	20,000

three E_{cm} regions. The data is observed to be consistent with the scaling behavior expected for γ 's from the decays of hadrons.)

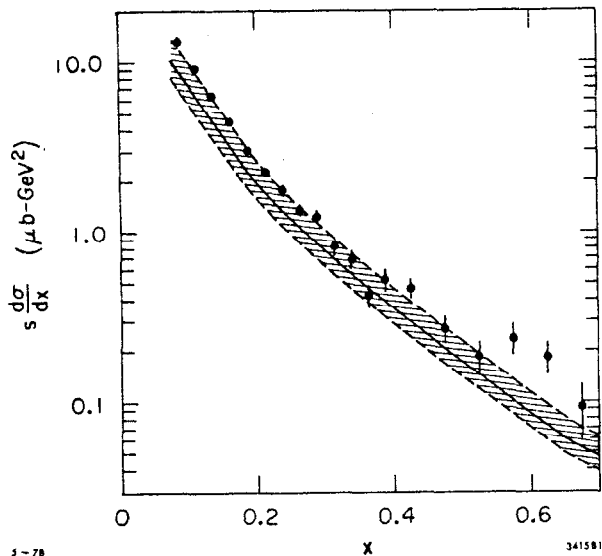


Fig. 3. Inclusive γ cross section for E_{cm} from 4.9 to 7.4 GeV. Curve represents the predicted cross section based on the assumptions that the π^0 cross section is half the observed charged- π cross section and π^0 's are the sole source of γ 's. Shaded region represents the estimated systematic error in the relative normalization.

Fig. 4. shows the invariant-mass distribution for all γ pairs with total momentum greater than 600 MeV/c. The dashed line is the estimated background obtained by combining γ pairs, where each γ is from a different event, and normalizing this distribution to the data in a mass interval above the π^0 mass.

The π^0 cross section is determined by independently subtracting the background in each momentum interval. The resulting inclusive cross section is shown in Fig. 5. The error bars include

the contribution from the uncertainty in the background subtraction. The curve is half the inclusive charged- π cross section⁵⁾ and the shaded region represents the estimated $\pm 20\%$ systematic error in the relative normalizations of the inclusive π^\pm and π^0 cross sections. Within errors, the two cross sections agree over

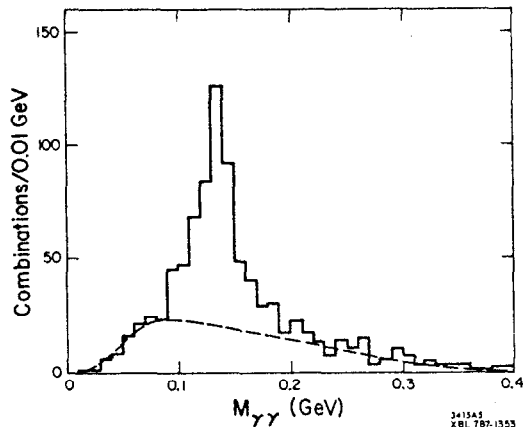


Fig. 4. Invariant-mass distribution for γ pairs with total momentum greater than 600 MeV/c. Background curve results from combinations taking γ 's from different events.

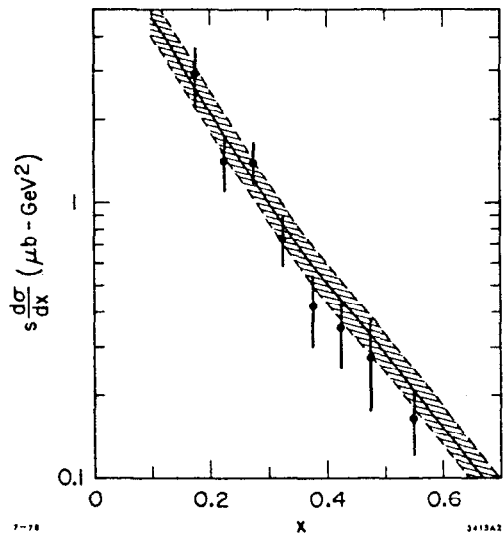


Fig. 5. Inclusive π^0 cross section as a function of x . Curve is half the charged- π cross section. Shaded region represents the uncertainty in the relative normalization.

the range of measurement. If these two inclusive cross sections are integrated over the region $x=0.15$ to $x=0.60$, the relative π^0 to π^\pm production is $\sigma(\pi^0) / [\sigma(\pi^+) + \sigma(\pi^-)] = 0.47 \pm 0.10$, where the error includes the $\pm 20\%$ systematic error in the relative normalizations.

It is of interest to determine whether the observed π^0 cross section can account for the observed γ production. Because of the large errors and limited x range of the π^0 production cross section, π^0 production was assumed to be equal to half the charged- π cross section shown in Fig. 5. From this, a γ spectrum is generated which is shown as the solid curve in Fig. 3. Again the shaded region represents the uncertainty in the relative normalizations. The observed γ cross section is possibly a little larger than, but consistent with, that expected from π^0 decay.

IV. Monte Carlo Analysis and Interpretation

The results of an analysis of inclusive charged particle production in e^+e^- annihilation by the SLAC-LBL Mark I magnetic detector collaboration¹⁾ is shown in Fig. 6. In the analysis, all particles were assumed to be pions. Acceptance and efficiency corrections were based on a limited transverse momentum jet model analysis. At high energy (i.e., above 5 GeV), the data appear to indicate that half the produced energy is going into production of neutrals, presumably π^0 's. However, the analysis just presented from the LGW experiment shows that the energy going into the production of π^0 's is only half that going into the production of charged π 's. Furthermore, there is no large excess of γ production above what is expected from the measured π^0 's to account for extra missing energy. Thus, the analyses appear to be in contradiction.

In an effort to understand this apparent inconsistency, the Lead-Glass Wall data was

analyzed in a manner similar to that used on the Mark I data presented in Ref. 1. Although the charged particle inclusive spectrum could be fit (and accounted for approximately half the produced energy) with the Monte Carlo model, the observed π^0 and γ distributions were approximately a factor of two below the Monte Carlo predictions. In order to try to obtain more consistent results, three major changes were made to the Monte Carlo model in an effort to make it more realistic.

First, the assumption that all particles are π 's was dropped. The relative fractions of K and nucleon production are known from previous measurements⁶⁾ and

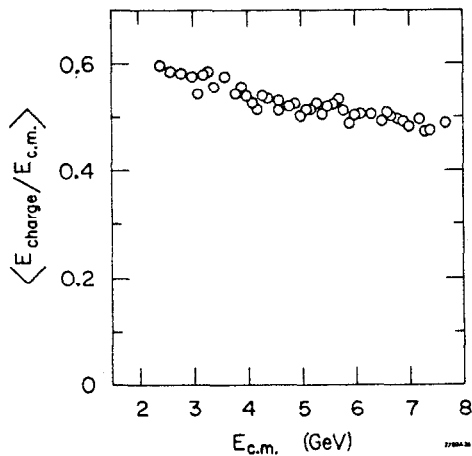


Fig. 6. Relative fraction of energy going into charged particle production as a function of $E_{\text{c.m.}}$. Data is from Ref. 1.

from the LGW data. Thus, K and nucleon production is included in the model in addition to π production. The advantage of including heavy particles is that some of the "missing energy" is really going into the rest mass of the heavier particles. For example, a particle with momentum 300 MeV/c has 330 MeV energy if it is a π , 580 MeV energy if it is a K, and 980 MeV energy if it is a proton. In the model, both neutral and charged K's and nucleons are included, with neutral production assumed to be equal to charged production. π^0 production is assumed to be half the charged π production, as measured in the LGW data.

Second, an additional component was added to the Monte Carlo consisting of $e^+e^- \rightarrow \tau^+\tau^-$ events (equal to 22% of the total hadronic cross section). τ decays produce a significant number of neutrinos, which contributes to the missing (unobserved) energy. Branching fractions used in the model were based on experimental results when available and on theoretical numbers otherwise.⁷⁾

Third, non-stable particles were included. This will tend to push the produced x distribution down to lower x since a primary particle of moderate energy will decay and yield low energy secondaries. Thus, the previous analysis which did not include non-stable particles underestimated the amount of energy going into the production of low momentum particles which were not detected by the apparatus. Ideally, one should include resonances such as η^0 's, ρ 's, and ω 's, and charmed particles like D's and F's. However, since the production (and in the case of charmed particles, also the decay) of these states is not well known, the inclusion of all such states in the model would lead to too many unknown and unconstrained parameters. Thus, it was decided to include only one "token" resonance, the η^0 , in the model. It was intended to take the place of all other resonances and weakly decaying particles. Thus, results relating to η^0 production are meaningless and have nothing to do with real η^0 's. The Monte Carlo has two undetermined quantities, the total produced multiplicity and the η^0 fraction. All other parameters are defined. These two parameters are varied until agreement is reached between the data and the Monte Carlo for the observed charged particle x distribution. This is done separately in each of the three E_{cm} regions shown in Table I. It should be noted that no information from the γ spectrum is used in the determination of the Monte Carlo parameters, and only after the parameters are determined from the charged particle data are the γ spectra compared.

Figure 7 shows a comparison between the data and the Monte Carlo for the observed charge multiplicity, the observed K^\pm multiplicity, and the observed \bar{p} multiplicity. Only data in the E_{cm} region from 6.9 to 7.4 GeV is shown. (The data in the other E_{cm} regions compare equally well.) The data points are the measured values. The dashed curves pass through the Monte Carlo points. The Monte Carlo provides an acceptable fit to the data. Fig. 8 shows the charged particle x distribution (observed and uncorrected) compared to the Monte Carlo

distribution for the highest E_{cm} region. Again the two distributions agree well.

Having established that the Monte Carlo model adequately describes the charged particle distributions, comparisons are made to the neutral distributions.

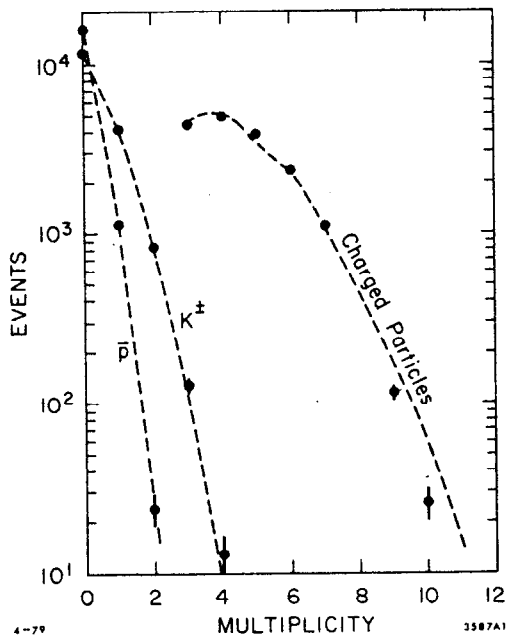


Fig. 7. Multiplicity distributions for all charged particles, charged K's, and \bar{p} 's. The data points are measured values for E_{cm} from 6.9 to 7.4 GeV. The dashed curves pass through the Monte Carlo values.

Fig. 9 shows the x distribution for γ 's. (The entire E_{cm} region from 4.9 to 7.4 GeV is included so that adequate statistics are available.) It is seen that the Monte Carlo predicts both the correct shape and normalization. In Fig. 10 the $\gamma\gamma$ invariant mass distribution for the same E_{cm} region is shown. There is a cut requiring the γ -pair momentum to be greater than 800 MeV/c. The dashed curve

Fig. 9. Inclusive γ distribution as a function of x for E_{cm} from 4.9 to 7.4 GeV. Dashed curve represents the Monte Carlo distribution.

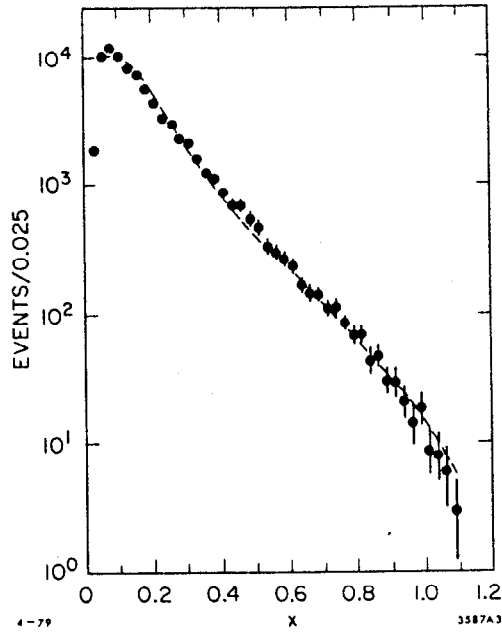


Fig. 8. Inclusive charged particle x distribution for E_{cm} from 6.9 to 7.4 GeV. Dashed curve represents the Monte Carlo distribution.

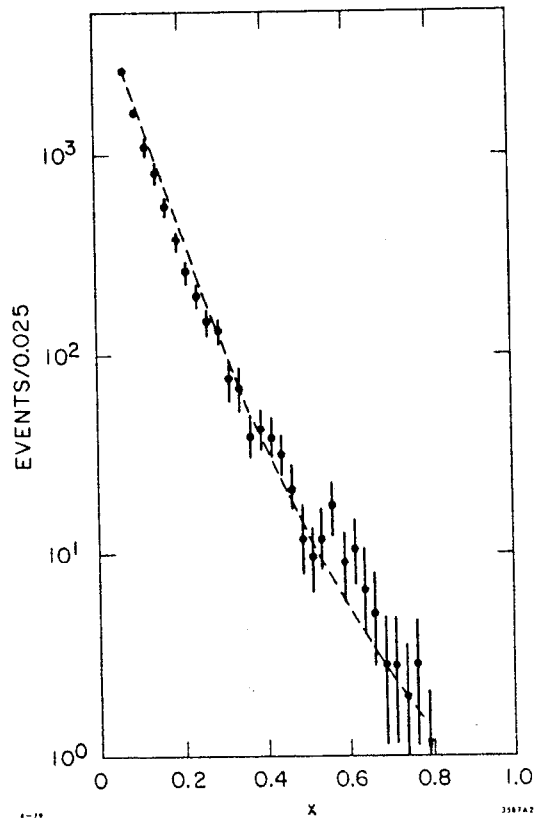
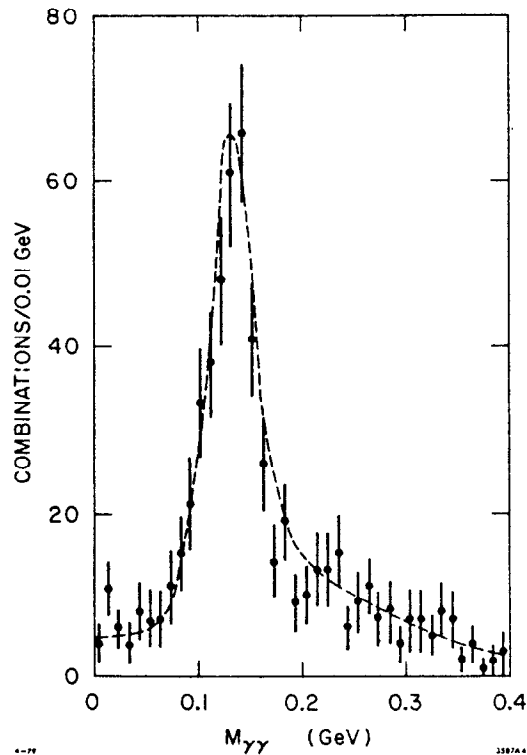


Fig. 10. $\gamma\gamma$ invariant mass distribution with $P_{\gamma\gamma} > 0.8$ GeV/c. Dashed curve is the Monte Carlo prediction.

shows the expected Monte Carlo distribution, which is consistent with the data.

The point of the analysis is that it is possible to construct a semi-realistic model for e^+e^- annihilation that accounts for all the measured charged and neutral particle distributions. There is no missing or unaccounted for energy, and hence, the "energy crisis" is just a manifestation of the model used in interpreting the data. No claim is made for the correctness of the model. It is consistent with everything that is known about particle production in e^+e^- annihilation, but very little is currently known about the production distribu-



tions of resonances and charmed particles. In addition, no claim is made regarding the uniqueness of the model. Significant variations in the parameters are allowed without seriously affecting the quality of the fit. Also, various changes to the model were made, such as including contributions from resonances other than the η^0 's (e.g., ρ 's and ω 's). It was generally possible to fit the data equally well with these models. Finally no claim is made regarding inclusive η^0 production. As stated earlier, the η^0 's included in the model are required to account for all decaying particles. In attempts with models which include other resonances, an in-

crease in one resonance fraction is reflected in a decrease in the others. For the sake of completeness, the relative multiplicities for the different particle types are given in Table II.

Table II. Monte Carlo produced multiplicity fractions as a function of center-of-mass energy.			
Particle Type	Monte Carlo Produced Multiplicity		
	4.9 - 6.0 GeV	6.0 - 6.9 GeV	6.9 - 7.4 GeV
$\pi^+ = \pi^- = \pi^0$	1.3	1.5	1.6
η^0	1.2	1.5	1.7
$K^\pm = K^0 + \bar{K}^0$.4	.4	.4
$p + \bar{p} = n + \bar{n}$.2	.2	.2
ν	.1	.1	.1
Total	6.5	7.2	7.6

REFERENCES

1. R. F. Schwitters, in Proceedings of the International Symposium on Lepton and Photon Interactions at High Energies, Stanford, California, 1975, ed., W. T. Kirk (Stanford Linear Accelerator Center, Stanford, California, 1975) p. 5.
2. D. L. Scharre et al., Phys. Rev. Lett. 41, 1005 (1978).
3. J.-E. Augustin et al., Phys. Rev. Lett. 34, 764 (1975).
4. J. M. Feller et al., IEEE Trans. Nucl. Sci. 25, 304 (1977).
5. This measurement is similar to previous measurements of the inclusive charged particle spectrum [see G. G. Hanson, in Proceedings of the Thirteenth Rencontre de Moriond on High-Energy Leptonic Interactions and High-Energy Hadronic Interactions, 1978, Vol. II, edited by Trân Thanh Vân (R.M.I.E.M. Orsay), p. 15.]. The major change involves elimination of tracks which are not pions. K's and p's are eliminated by time-of-flight separation. (At higher momentum, the separation is based on extrapolation from the lower-momentum data.) Muon and electron contamination (on the order of a few percent) is corrected for in the Monte Carlo acceptance calculation.
6. See for example V. Lüth et al., Phys. Lett. 70B, 120 (1977); M. Piccolo et al., Phys. Rev. Lett. 39, 1503 (1977); R. Brandelik et al., DESY 78/50 (1978), unpublished.
7. The relevant numbers are reviewed in M. L. Perl, in Proceedings of the Advanced Summer Institute 1978 (University of Karlsruhe, Karlsruhe, 1978), to be published.